

Supplementary Materials for

Rapid depletion of ESCRT protein Vps4 underlies injury-induced autophagic impediment and Wallerian degeneration

Haiqiong Wang, Xuejie Wang, Kai Zhang, Qingyao Wang, Xu Cao, Zhao Wang, Shuang Zhang, Ang Li*, Kai Liu*, Yanshan Fang*

*Corresponding author. Email: anglijnu@jnu.edu.cn (A.L.); kailiu@ust.hk (K.L.); fangys@sioc.ac.cn (Y.F.)

Published 13 February 2019, *Sci. Adv.* **5**, eaav4971 (2019)
DOI: 10.1126/sciadv.aav4971

This PDF file includes:

Fig. S1. The evaluation system of wing axonal degeneration scores.

Fig. S2. The ESCRT-I component TSG101 is required but not sufficient to maintain axonal integrity.

Fig. S3. Axon injury induces a rapid autophagy response followed by axonal destruction.

Fig. S4. Inhibition of autophagy induction by RNAi-*Atg12* or RNAi-*Atg17* provides moderate axonal protection.

Fig. S5. Examination of endogenous Vps4B protein and lentiviral OE of Vps4B in mouse DRG neurons.

SUPPLEMENTARY FIGURES

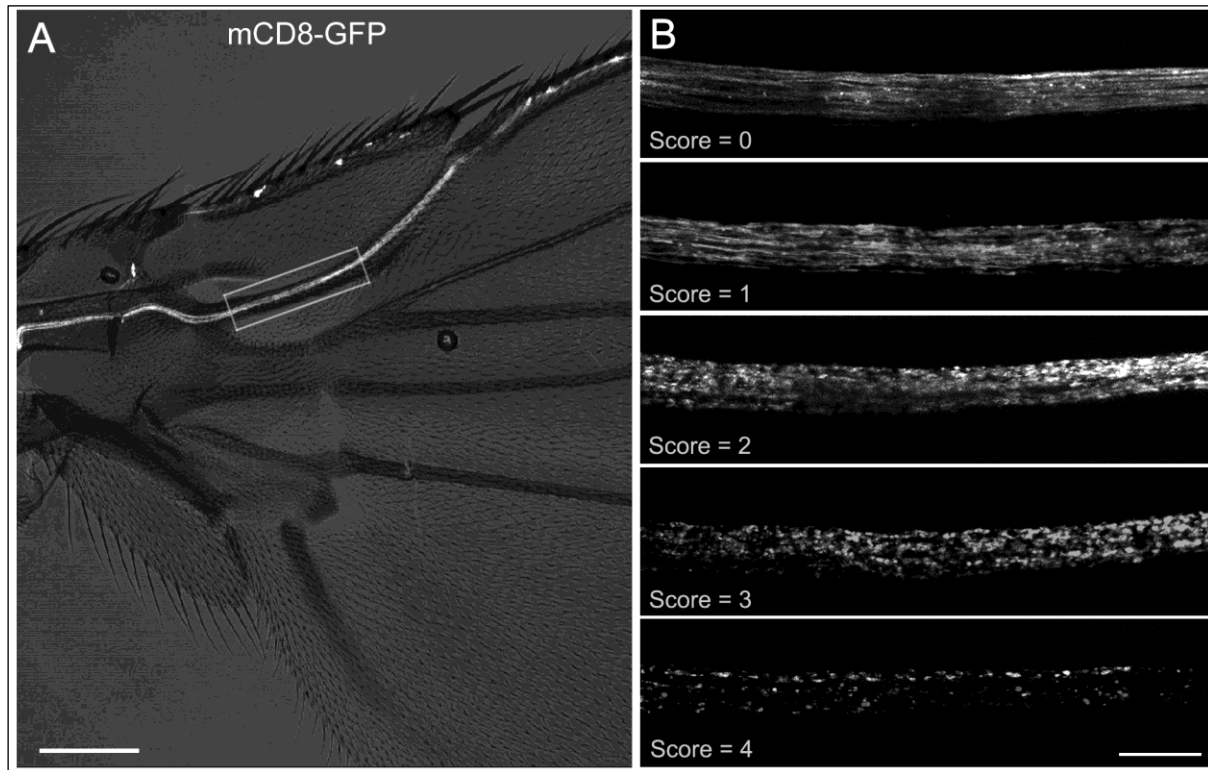


Fig. S1. The evaluation system of wing axonal degeneration scores. (A) The axonal integrity was assessed using mCD8-GFP as a marker and quantified as previously described (22,23). The boxed area of the fly wing nerve is imaged and assessed in this study using the evaluation system in (B). **(B)** Representative images of the wing nerve with indicated axonal degeneration scores. Specifically, in intact axons, continuous, smooth, fiber-like mCD8-GFP signal is seen (degeneration score 0). After injury, axonal mCD8-GFP starts to show beading (degeneration score 1), fragmentation (degeneration score 2), discontinued axons (degeneration score 3), and finally the fluorescent intensity is dramatically decreased (degeneration score 4). Scale bars: 50 μm in (A) and 20 μm in (B).

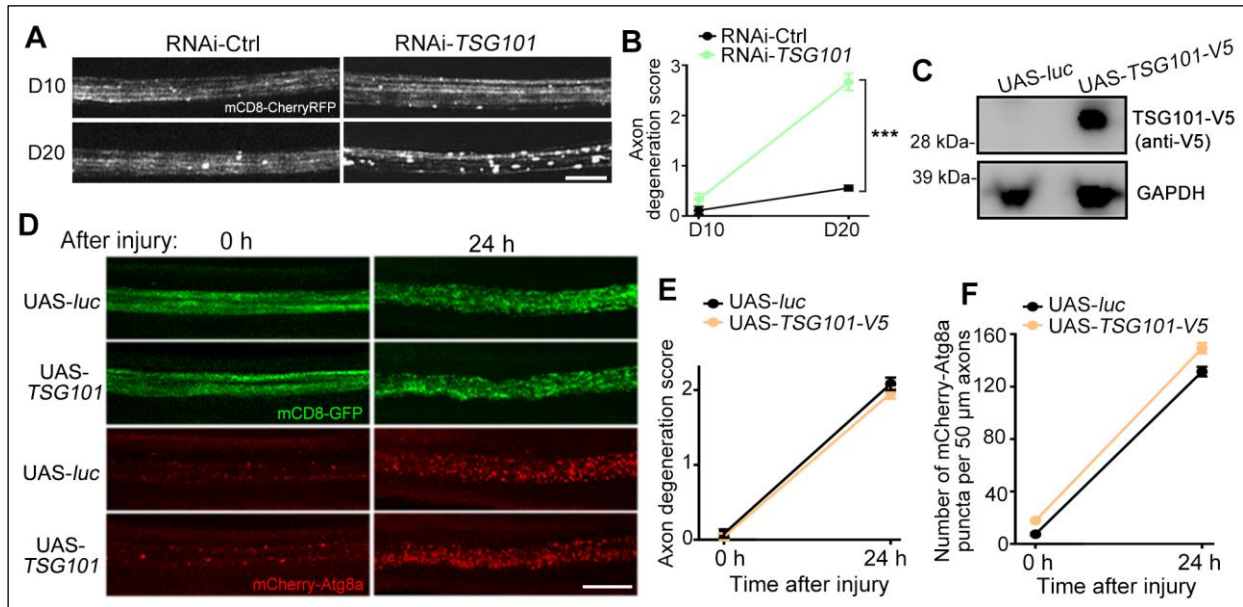


Fig. S2. The ESCRT-I component TSG101 is required but not sufficient to maintain axonal integrity. (A-B) Representative images (A) and quantification (B) of wing axons labeled by mCD8-CherryRFP of RNAi-Ctrl (RNAi-*luc*) or RNAi-*TSG101* flies at indicated time points. (C) Representative Western blots confirming overexpression of V5 tagged TSG101 in the UAS transgenic flies that we generated. (D-F) Representative images (D) and quantifications (E-F) of wing axons labeled by mCD8-GFP for axonal integrity and mCherry-Atg8a for autophagy at indicated time points after injury. Data are shown as mean \pm SEM; $n = 8\text{--}12$ wings per time point per group. *** $P < 0.001$; two-way ANOVA. Scale bars: 10 μm .

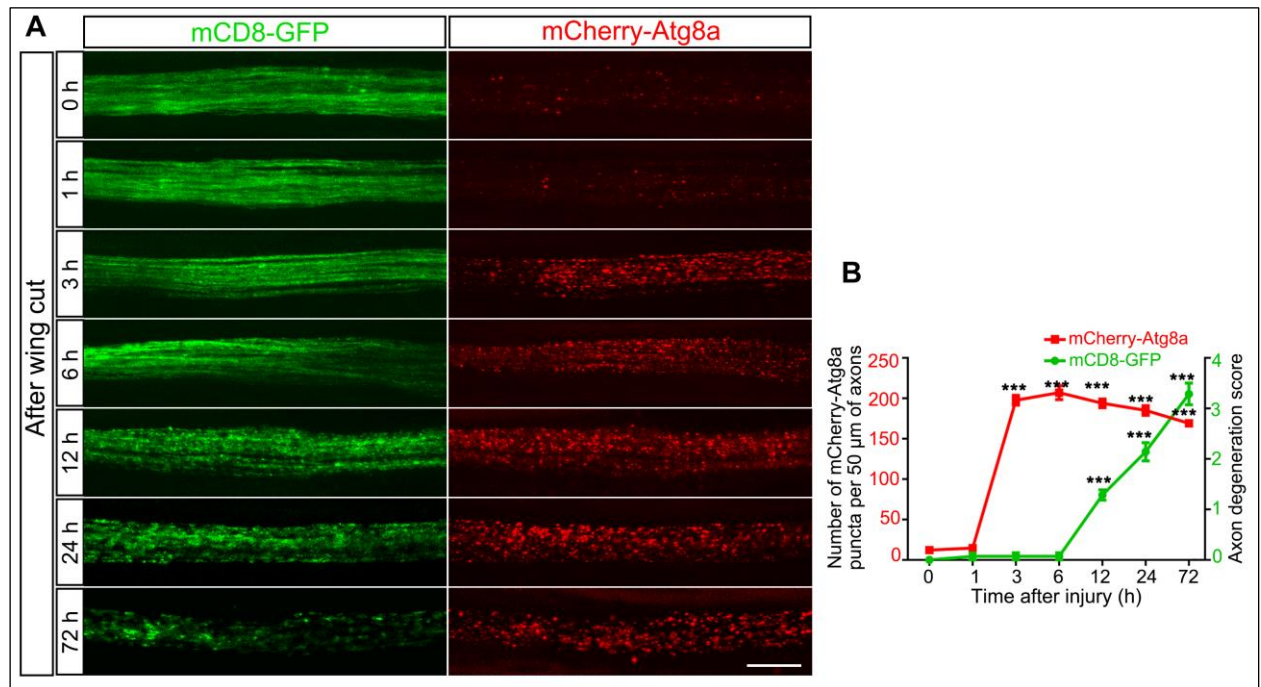


Fig. S3. Axon injury induces a rapid autophagy response followed by axonal destruction.

(A) Representative confocal images of the wing axons highlighted by mCD8-GFP for axonal integrity and mCherry-Atg8a for autophagy levels at indicated time points after a wing cut.

Significant increase of mCherry-Atg8a puncta can be seen as early as 3 h after axotomy, whereas marked axonal fragmentation is not observed until 12 h after injury. (B) Quantifications of the severity of axonal degeneration and the levels of autophagy in (A). The axonal degeneration scores are assessed as described in Figure S1 and the autophagy levels are evaluated as average numbers of mCherry-Atg8a puncta per 50 μm of axons. Mean \pm SEM; $n = 7\sim 10$ wings per time point; $***P < 0.001$; Student's t -test, significance is compared to 0 h. Scale bar: 10 μm .

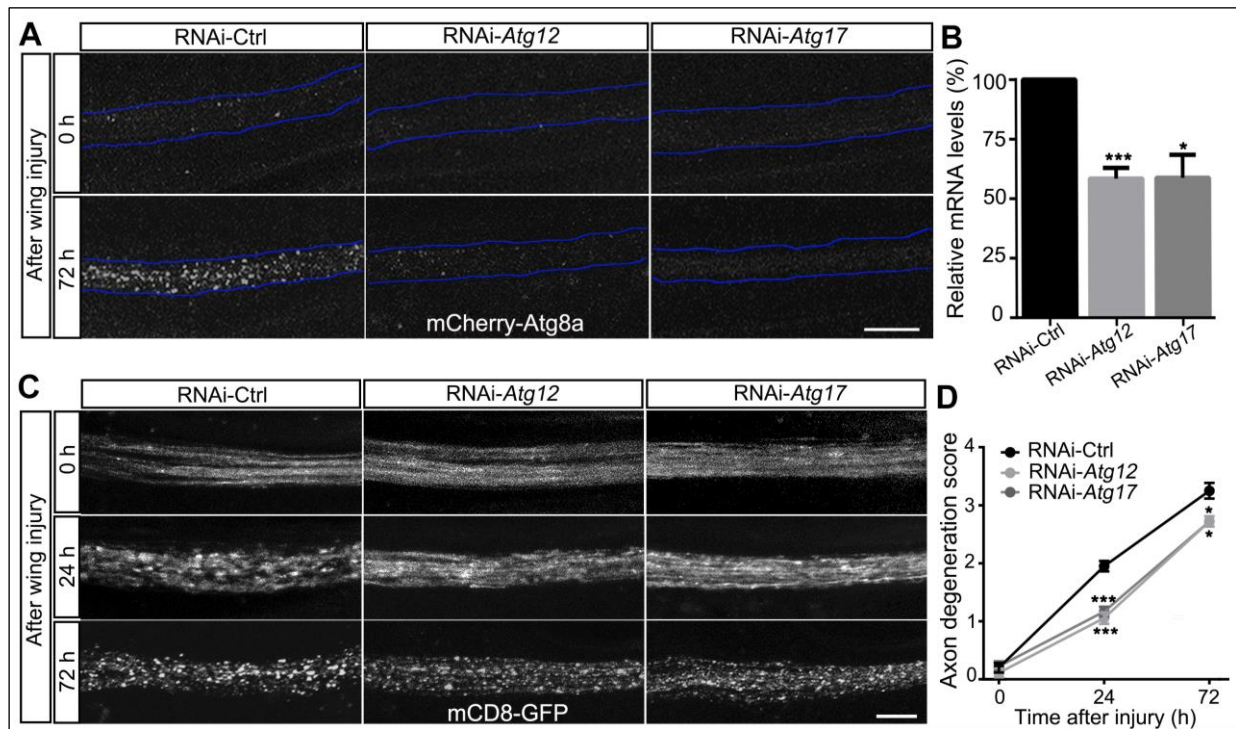


Fig. S4. Inhibition of autophagy induction by RNAi-Atg12 or RNAi-Atg17 provides moderate axonal protection. (A) Representative images of wing nerve (within the blue outlines) labeled by mCherry-Atg8a at indicated time points after injury. Downregulation of *Atg12* or *Atg17*, the core Atg genes required for phagophore assembly and autophagosome formation, sustainably suppresses the induction of mCherry-Atg8a puncta in injured axons. (B) The knockdown efficiency of RNAi-*Atg12* and RNAi-*Atg17* is analyzed by qPCR and normalized to *actin*. Data shown are mean \pm SEM; $n = 3$; * $p < 0.05$, *** $p < 0.001$; Student's *t*-test. (C) The integrity of severed axons of RNAi-*Atg12* or RNAi-*Atg17* flies is evidently better than that of the RNAi-Ctrl group at 24 h after injury; by 72 h, however, the majority of the injured axons of the RNAi-*Atg12* and RNAi-*Atg17* flies have degenerated and the axonal integrity is only slightly better than that of the RNAi-Ctrl group. (D) Quantification of axonal degeneration scores in A. Data are mean \pm SEM, $n = 9\text{--}10$ per group; * $P < 0.05$, *** $P < 0.001$; Student's *t*-test compared to the RNAi-Ctrl group at each time point. Scale bars: 10 μm .

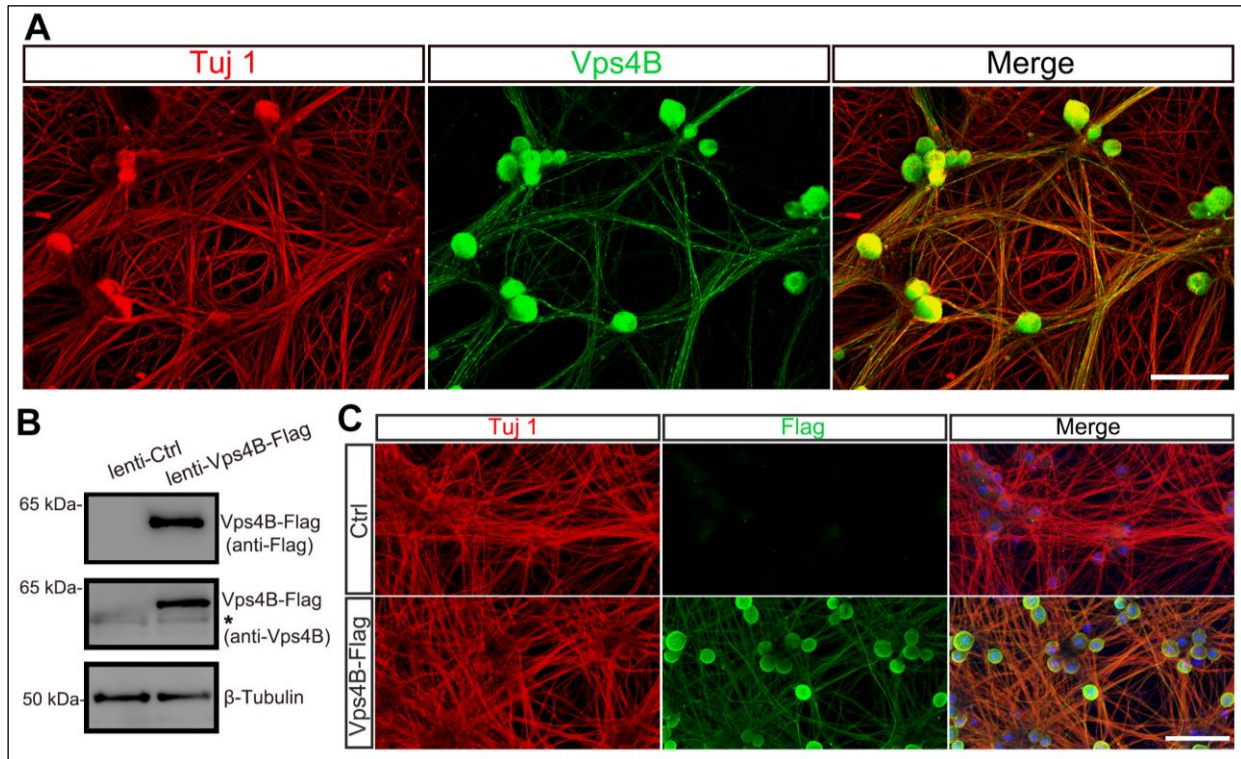


Fig. S5. Examination of endogenous Vps4B protein and lentiviral OE of Vps4B in mouse

DRG neurons. (A) Immunostaining of *in vitro* cultured C57BL/6 mouse E14 DRG neurons.

Vps4B (green) is expressed in both soma and neurites. Neuron-specific class III β -tubulin (Tuj 1, red), a neuronal marker to label axons and the cytoplasm of soma. (B) Western blot analysis

confirming Vps4B OE in DRG neurons by lenti-Vps4B-Flag infection. Asterisk, endogenous mouse Vps4B. (C) Representative fluorescent images of the DRG neuron cultures used in Fig.

3A-3B. Mouse E14 DRG neurons are cultured *in vitro* for 7 days and then infected with lenti-

Vps4B-flag for 7~10 days. Tuj 1 (red), Flag (green) and a merge of all channels with DAPI (stain

the nucleus, blue) are shown. Scale bars: 100 μ m.